



HAL
open science

Effects of Red Sorghum-Derived Deoxyanthocyanidins and Their O- β -D-Glucosides on E-Cadherin Promoter Activity in PC-3 Prostate Cancer Cells

Nathalie Mora, Maxence Rosa, Mohamed Touaibia, Luc J Martin

► **To cite this version:**

Nathalie Mora, Maxence Rosa, Mohamed Touaibia, Luc J Martin. Effects of Red Sorghum-Derived Deoxyanthocyanidins and Their O- β -D-Glucosides on E-Cadherin Promoter Activity in PC-3 Prostate Cancer Cells. *Molecules*, 2024, 29, 10.3390/molecules29081891 . hal-04802535

HAL Id: hal-04802535

<https://hal.inrae.fr/hal-04802535v1>

Submitted on 25 Nov 2024

HAL is a multi-disciplinary open access archive for the deposit and dissemination of scientific research documents, whether they are published or not. The documents may come from teaching and research institutions in France or abroad, or from public or private research centers.

L'archive ouverte pluridisciplinaire **HAL**, est destinée au dépôt et à la diffusion de documents scientifiques de niveau recherche, publiés ou non, émanant des établissements d'enseignement et de recherche français ou étrangers, des laboratoires publics ou privés.



Distributed under a Creative Commons Attribution 4.0 International License

Article

Effects of Red Sorghum-Derived Deoxyanthocyanidins and Their O- β -D-Glucosides on E-Cadherin Promoter Activity in PC-3 Prostate Cancer Cells

Nathalie Mora ¹, Maxence Rosa ¹, Mohamed Touaibia ²  and Luc J. Martin ^{3,*} 

¹ UMR408 INRA–UAPV, SQPO, Qualim, University Avignon, Campus Jean-Henri Fabre, Pôle Agrosciences, 301, Rue Baruch de Spinoza, 84911 Avignon, France; nathalie.mora@univ-avignon.fr (N.M.); maxence.rosa@univ-avignon.fr (M.R.)

² Chemistry and Biochemistry Department, Université de Moncton, Moncton, NB E1A 3E9, Canada; mohamed.touaibia@umoncton.ca

³ Biology Department, Université de Moncton, Moncton, NB E1A 3E9, Canada

* Correspondence: luc.martin@umoncton.ca

Abstract: Although much less common than anthocyanins, 3-Deoxyanthocyanidins (3-DAs) and their glucosides can be found in cereals such as red sorghum. It is speculated that their bioavailability is higher than that of anthocyanins. Thus far, little is known regarding the therapeutic effects of 3-DAs and their O- β -D-glucosides on cancer, including prostate cancer. Thus, we evaluated their potential to decrease cell viability, to modulate the activity of transcription factors such as NF κ B, CREB, and SOX, and to regulate the expression of the gene *CDH1*, encoding E-Cadherin. We found that 4',7-dihydroxyflavylium chloride (P7) and the natural apigeninidin can reduce cell viability, whereas 4',7-dihydroxyflavylium chloride (P7) and 4'-hydroxy-7-O- β -D-glucopyranosyloxyflavylium chloride (P3) increase the activities of NF κ B, CREB, and SOX transcription factors, leading to the upregulation of *CDH1* promoter activity in PC-3 prostate cancer cells. Thus, these compounds may contribute to the inhibition of the epithelial-to-mesenchymal transition in cancer cells and prevent the metastatic activity of more aggressive forms of androgen-resistant prostate cancer.

Keywords: 3-deoxyanthocyanidin; 3-deoxyanthocyanin; PC-3 cells; transcription factors; E-cadherin



Citation: Mora, N.; Rosa, M.; Touaibia, M.; Martin, L.J. Effects of Red Sorghum-Derived Deoxyanthocyanidins and Their O- β -D-Glucosides on E-Cadherin Promoter Activity in PC-3 Prostate Cancer Cells. *Molecules* **2024**, *29*, 1891. <https://doi.org/10.3390/molecules29081891>

Academic Editors: Rosalva Mora-Escobedo, Cristian Jiménez Martínez and Mercedes Martín Pedrosa

Received: 18 March 2024

Revised: 16 April 2024

Accepted: 20 April 2024

Published: 21 April 2024

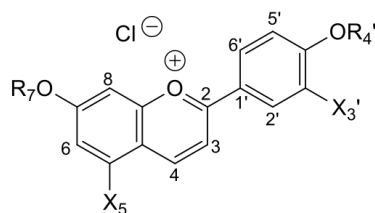


Copyright: © 2024 by the authors. Licensee MDPI, Basel, Switzerland. This article is an open access article distributed under the terms and conditions of the Creative Commons Attribution (CC BY) license (<https://creativecommons.org/licenses/by/4.0/>).

1. Introduction

The colors of flowers, fruits, vegetables, and cereals can be attributed to their content in anthocyanins and vary from red to blue according to pH, self-association, and interactions with phenolic copigments, such as flavonols, flavones, and hydroxycinnamic acids, and metal ions (Al³⁺, Fe³⁺, Mg²⁺) [1–3]. Anthocyanins were found to be a subclass of flavonoids present in many flowers, fruits, and vegetables, as well as in fruit-based beverages, notably red wine. Because of their natural coloring properties, anthocyanins make a major contribution to the quality and consumer appeal of food. They can also be associated with the health benefits of a diet rich in plant products [4].

Cereals such as red sorghum are an important source of 3-deoxyanthocyanidins (3-DA) and their glucosides [5]. 3-Deoxyanthocyanidins are more stable than anthocyanidins because of their absence of a C3-OH group, which plays an essential role in their degradation [6]. Under slightly acidic to neutral conditions, 3-DAs have more intense and more stable colors than common anthocyanins. Indeed, the absence of the OH group on C3 makes these pigments considerably less sensitive to the addition of water at C2 [7,8] (see Scheme 1), which makes them more resistant to irreversible chemical degradation and reversibly leads to colorless hemiketal and chalcone forms [9].



Pigment	X _{3'}	R _{4'}	X ₅	R ₇	Yield (%) ^a
P1	OH	H	H	H	56
P2	OH	H	H	β-D-Glc	75 ^b
P3	H	H	H	β-D-Glc	42 ^b
P5	H	β-D-Glc	H	H	77
P6	H	β-D-Glc	H	Me	77
P7	H	H	H	H	45
APN	H	H	OH	H	78

^a Yield of isolated pigments in the condensation step; ^b Yield also includes the step of sugar deprotection.

Scheme 1. Pigments investigated.

These pigments (3-DA) are also promising for their potential health benefits, expressed through cell-specific antioxidant effects [10–12]. Moreover, their bioavailability could be expected to be better than that of anthocyanins. Indeed, 3-deoxyanthocyanidins are probably less subject to catabolism in the gastrointestinal tract. To date, little is known about the therapeutic effects of 3-DAs and their O-β-D-glucosides on cancer, including prostate cancer.

In our recent work, we reported the chemical synthesis of 3-DAs and their O-β-D-glucosides (Scheme 1), including the typical sorghum red natural pigments apigeninidin (APN, 4',5,7-trihydroxyflavylium) and luteolinidin (LTN, 3',4',5,7-tetrahydroxyflavylium) [13,14]. However, the possible therapeutic effects of these 3-DAs and their O-β-D-glucosides on cancer, including prostate cancer, are not well known.

Mainly diagnosed in men over 50, prostate cancer has favorable 5-year survival rates as a result of early detection and the availability of curative surgery. However, progression to a more aggressive form resistant to androgen deprivation and with increased metastatic activity is responsible for the majority of deaths associated with prostate cancer. Thus, alternative treatments for prostate cancer are worth considering and could involve the use of 3-DAs and their O-β-D-glucosides.

Transcription factors are DNA-binding proteins with a sequence-specific DNA-binding domain and an activation/repression domain, which interacts with multiple coregulators, contributing to the recruitment of RNA polymerase II. Transcription factors can act as activators or repressors of transcription, depending on the cofactors and chromatin modulators recruited [15]. Changes in the activity of transcription factors are associated with the development or prevention of various diseases, including prostate cancer. In addition to the androgen receptor, other transcription factors are involved in regulating various cancer properties associated with prostate tumorigenesis. Among these, the cyclic AMP response element (CRE)-binding protein (CREB), the SRY-box transcription factors (SOX), and the nuclear factor kappa-light-chain-enhancer of activated B cells (NFκB) have been characterized as regulators of gene expression influencing prostate cancer progressions [16–18].

Among the different types of molecules that keep cells together, cadherins play an important role in the formation of adherens junctions, thus mediating calcium-dependent cell-cell adhesion [19]. During the development of aggressive cancer, the epithelial-to-mesenchymal transition (EMT), characterized by a change in the expression from E-cadherin (CDH1) to N-cadherin (CDH2), enables cancer cells to acquire invasive and metastatic properties [20,21]. Indeed, the potential for prostate cancer invasiveness and metastasis

is suppressed by the over-expression of *CDH1* [22]. Interestingly, the activation of CREB transcription factors by protein kinase A has been associated with a mesenchymal-to-epithelial transition as a result of increased *CDH1* expression [23]. NF κ B activation has been linked to the inhibition of *CDH1* expression [24], thus promoting EMT of prostate cancer cells. Members of the SOX family can be divided into transcriptional activators and repressors [25]. Hence, depending on which SOX factors are expressed in cancer cells, they may have an activating or inhibitory effect on *CDH1* expression.

The aim of this work is to study the structure–activity relationships of synthesized pigments, including 3-DAs and their O- β -D-glucosides, on cell viability and gene regulation related to the epithelial-to-mesenchymal transition in the androgen-resistant prostate cancer cell line PC-3.

2. Results

2.1. Effects of Synthesized Pigments on Cell Viability

The chemical structures of the synthesized pigments assessed for their effects on the viability of PC-3 prostate cancer cells and the expression of *CDH1*-related genes are presented in Scheme 1.

To better assess the structure–activity relationship of the synthesized pigments and their anti-cancer properties against prostate cancer, the viability of androgen-resistant PC-3 prostate cancer cells was first evaluated following 24 h treatments with increasing concentrations of the molecules (Figure 1). Interestingly, treatment with the P1 molecule resulted in a reduction in PC-3 cell viability by 40% at 100 μ M and by 54% at 500 μ M (Figure 1a). The P2 molecule resulted in a modest reduction in cell viability by 20% at 500 μ M, while the P7 molecule decreased cell viability by 46% at 500 μ M (Figure 1b,f). The OH at position 3', as in the P1 molecule, seems to be decisive for the reduction in cell viability. Glycosylation at position 7 (P2 molecule) and the absence of the hydroxyl group at position 3' (P7 molecule) do not have a significant effect on the reduction in the viability of PC-3 cells (Figure 1b,f).

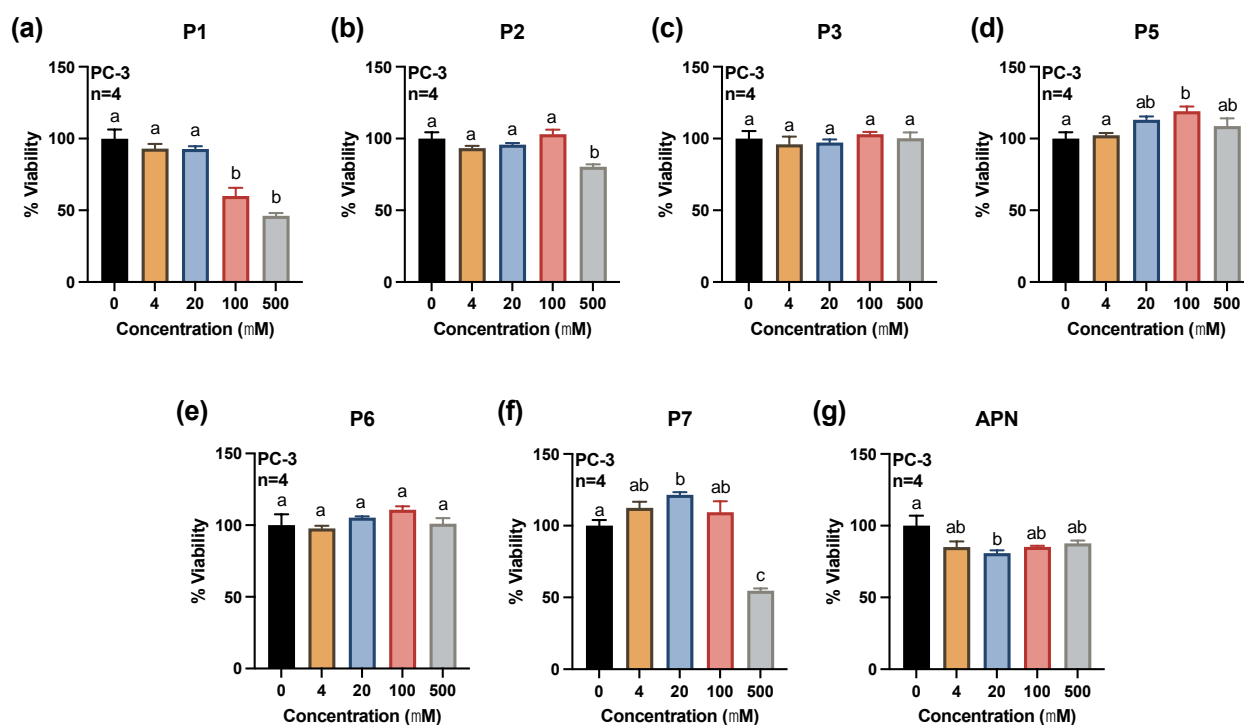


Figure 1. Viability of PC-3 prostate cancer cells in response to treatments with the indicated molecules. Cells were incubated in the absence or presence of increasing concentrations (0, 4, 20, 100, 500 μ M) of

the indicated molecules for 24 h, followed by the determination of cell viability as described in the Material and Methods Section. Results for the viability of PC-3 cells following treatments with P1 (a), P2 (b), P3 (c), P5 (d), P6 (e), P7 (f), and APN (g) are presented. The experiments were repeated four times, and the results are presented as percent cell viability over control (0 μ M, DMSO only) (\pm SEM). Statistical comparisons were performed using a one-way ANOVA followed by a Holm-Sidak multiple comparison test, where different letters denote significant differences ($p < 0.05$).

Compared with the P5 molecule, the addition of a methyl moiety at position 7 has no influence on cell viability, as demonstrated with the P6 molecule for all tested concentrations (Figure 1e).

Although the APN molecule appears to decrease the viability of PC-3 cells at all the concentrations evaluated, only the concentration of 20 μ M resulted in a significant reduction of 19% (Figure 1g). As shown by the effect of APN, the presence of a hydroxyl at position 5 is more decisive for a better reduction in PC-3 cell viability.

2.2. Influences of Synthesized Pigments on the Expression of E-Cadherin-Related Genes

To better define the potential influence of synthesized pigments on the regulation of gene expression in prostate cancer cells, different reporter plasmid constructs harboring the consensus regulatory elements for NF κ B, CREB, or SOX were transfected in PC-3 cells followed by treatments for 24 h with increasing concentrations of the molecules. Interestingly, treatment with the P1 molecule increased the activity of NF κ B transcription factors by 1.27 folds at 100 μ M (Figure 2a), while the P3 molecule resulted in increases by 1.24 folds at 100 μ M and by 1.28 folds at 500 μ M (Figure 2c). In addition, the P7 molecule increased the activity of NF κ B transcription factors by more than 1.23 folds at concentrations from 20 to 500 μ M (Figure 2e). The presence or absence of the hydroxyl or the D-glycosyl moieties at positions 3' or 7 leads to increased activity of NF κ B transcription factors. Oppositely, the APN molecule bearing only a hydroxyl moiety at position 5' was the only pigment that significantly decreased the activity of NF κ B transcription factors by 33% at 500 μ M (Figure 2f).

Regarding the influence of synthesized pigments on the activity of CREB transcription factors, PC-3 prostate cancer cells were transfected with a reporter plasmid construct harboring CREB consensus regulatory elements followed by treatments for 24 h with increasing concentrations of the molecules (Figure 3). Interestingly, treatment with the P2 molecule increased the activity of CREB transcription factors by 1.37 and 1.31 folds at 10 and 500 μ M, respectively (Figure 3b). The activity of CREB transcription factors was also increased by more than 1.42 folds following treatments with the P3 molecule at concentrations of 100 and 500 μ M (Figure 3c), as well as by 1.52 folds in response to treatment with the P5 molecule at 10 μ M (Figure 3d). Treatment with the P7 molecule also increased the activity of CREB transcription factors by more than 1.40 folds at concentrations of 100 and 500 μ M (Figure 3e), whereas treatment with the APN molecule resulted in an increase by more than 1.36 folds at concentrations ranging from 10 to 100 μ M (Figure 3f).

In contrast to the effect on the activity of NF κ B transcription factors, molecules P2, P3, P5, P7, and APN increased the activity of CREB transcription factors.

To evaluate the influence of the synthesized pigments on the activity of SOX transcription factors, PC-3 prostate cancer cells were transfected with a reporter plasmid construct harboring SOX consensus regulatory elements followed by treatments with increasing concentrations of the molecules for 24 h (Figure 4). This SOX DNA regulatory element can interact with SOX4, 5, 8, 9, 10, 12, 13, 14, 15, 17, or 18. According to RNA-Seq data from PC-3 cells [26], the SOX members SOX4, 9, 12, 13, 15, 17, and 18 are expressed in this cell model and can be redundant in regulating pSOX-luc activity. Although treatment with the P1 molecule increased the activity of SOX transcription factors by 1.18 folds at 100 μ M, such activity was decreased by 24% at 500 μ M (Figure 4a). The activity of SOX transcription factors was increased by more than 1.18 folds following treatments with the P3 molecule at concentrations of 10, 100, and 500 μ M (Figure 4c), as well as by more than 1.34 folds in response to treatment with the P7 molecule at 10 or 100 μ M (Figure 4e). However, treatment

with the APN molecule decreased the activity of SOX transcription factors in PC-3 cells by 22% at 500 μ M (Figure 4f).

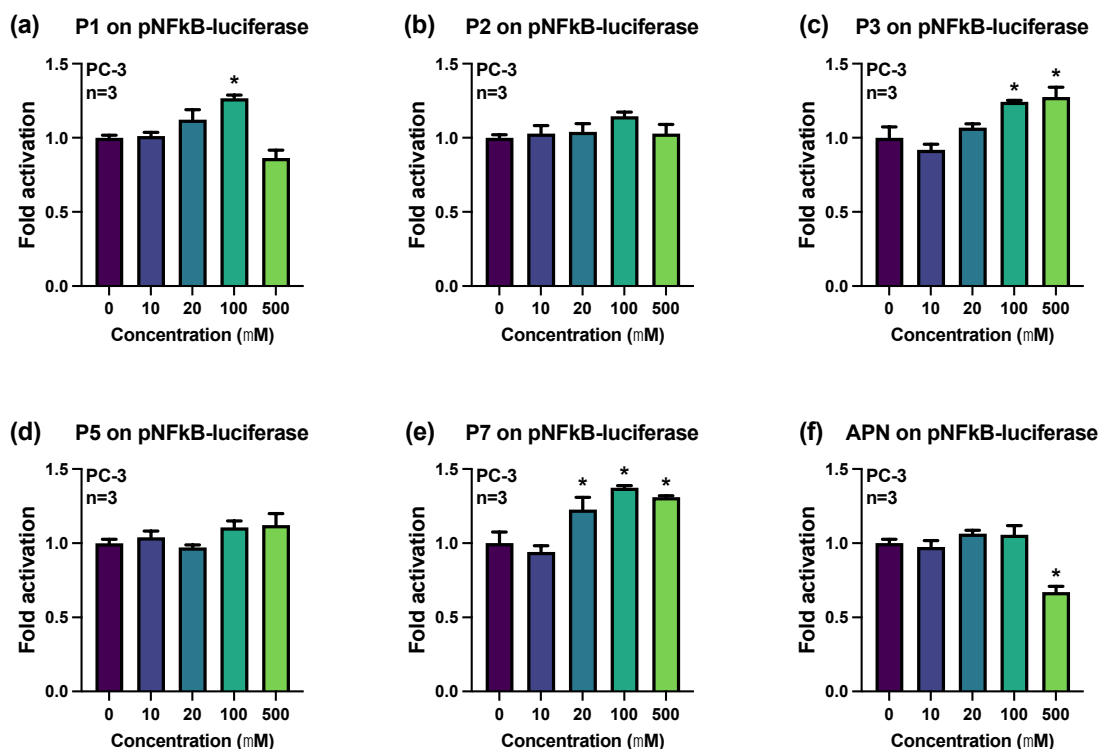


Figure 2. Effects of the indicated molecules on the activity of NFκB transcription factors. PC-3 prostate cancer cells were transfected with a luciferase plasmid reporter harboring four consensus NFκB regulatory elements upstream of the gene encoding *Firefly* luciferase. Cells were treated with increasing concentrations of the indicated molecules for 6 h. Results for the activation of the NFκB transcription factors following treatments of PC-3 cells with P1 (a), P2 (b), P3 (c), P5 (d), P7 (e), and APN (f) are presented. Results are presented as fold activation over the control (DMSO only) (\pm SEM). A one-way ANOVA was used to analyze data according to the concentrations of the indicated molecules, followed by Dunnett's multiple comparison test for significant differences compared to the control (* $p < 0.05$).

As with the effect on the activity of NFκB transcription factor, molecules P2, P3, P5, and P7 increased the activity of SOX transcription factors. As for NFκB activity, APN is the only molecule that decreases the activity of SOX transcription factors.

Since the activity of the *CDH1* gene promoter can be influenced by the presence and changes in the activity of the NFκB, CREB, and SOX transcription factors [27], we evaluated the potential effects of synthesized pigments on the regulation of the human -670 to $+92$ bp *CDH1* promoter region (Figure 5). Interestingly, treatment with the P3 molecule activated the *CDH1* promoter by 1.31 and 1.21 folds at 100 and 500 μ M, respectively (Figure 5c), while treatment with the P7 molecule resulted in an increase of 1.36 folds at 100 μ M (Figure 5e). The P7 molecule or its glycosylated analog (P3) at position 7 were the only molecules with an activating effect on this gene. The presence of a hydroxyl at the 3' and 5' positions and a glycosyl at the 4' position had no effect on this gene's activation.

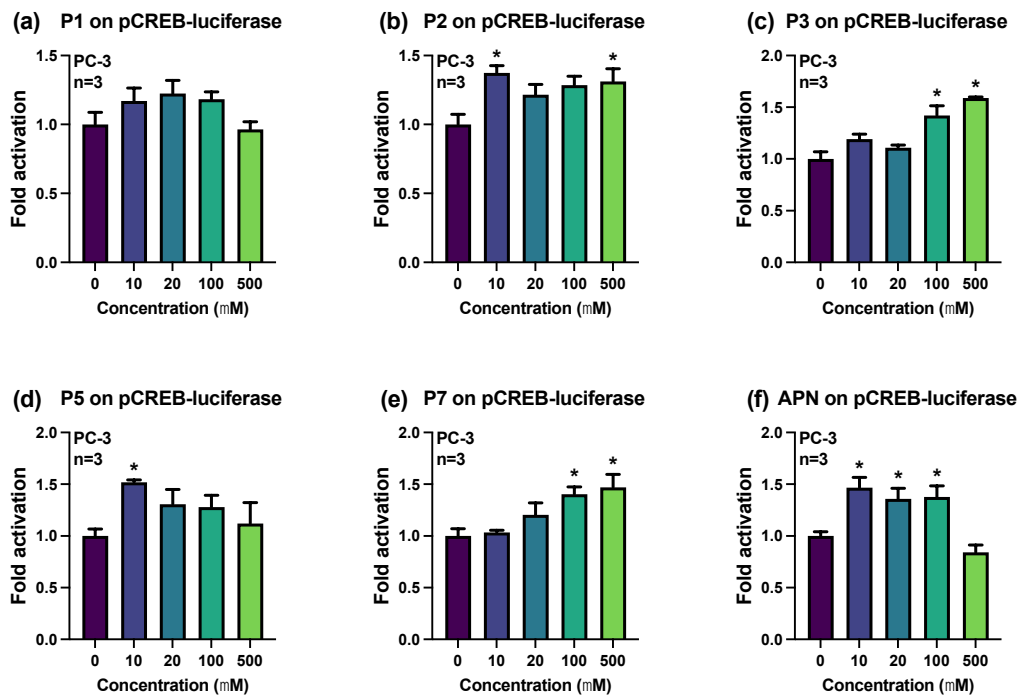


Figure 3. Effects of the indicated molecules on the activity of CREB transcription factors. PC-3 prostate cancer cells were transfected with a luciferase plasmid reporter harboring four consensus CREB regulatory elements upstream of the gene encoding *Firefly* luciferase. Cells were treated with increasing concentrations of the indicated molecules for 6 h. Results for the activation of the CREB transcription factors following treatments of PC-3 cells with P1 (a), P2 (b), P3 (c), P5 (d), P7 (e), and APN (f) are presented. Results are presented as fold activation over the control (DMSO only) (\pm SEM). A one-way ANOVA was used to analyze data according to the concentrations of the indicated molecules, followed by Dunnett's multiple comparison test for significant differences compared to the control (* $p < 0.05$).

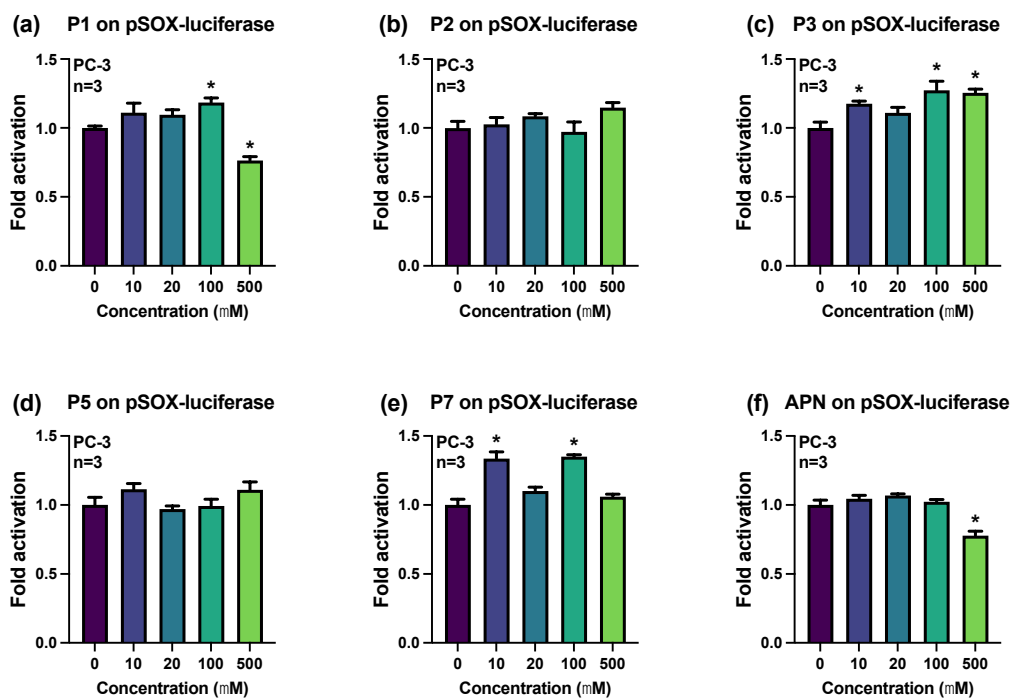


Figure 4. Effects of the indicated molecules on the activity of SOX transcription factors. PC-3 prostate cancer cells were transfected with a luciferase plasmid reporter harboring four consensus SOX regulatory

elements upstream of the gene encoding *Firefly* luciferase. Cells were treated with increasing concentrations of the indicated molecules for 6 h. Results for the activation of SOX transcription factors following treatments of PC-3 cells with P1 (a), P2 (b), P3 (c), P5 (d), P7 (e), and APN (f) are presented. Results are presented as fold activation over the control (DMSO only) (\pm SEM). A one-way ANOVA was used to analyze data according to the concentrations of the indicated molecules, followed by Dunnett's multiple comparison test for significant differences compared to the control ($* p < 0.05$).

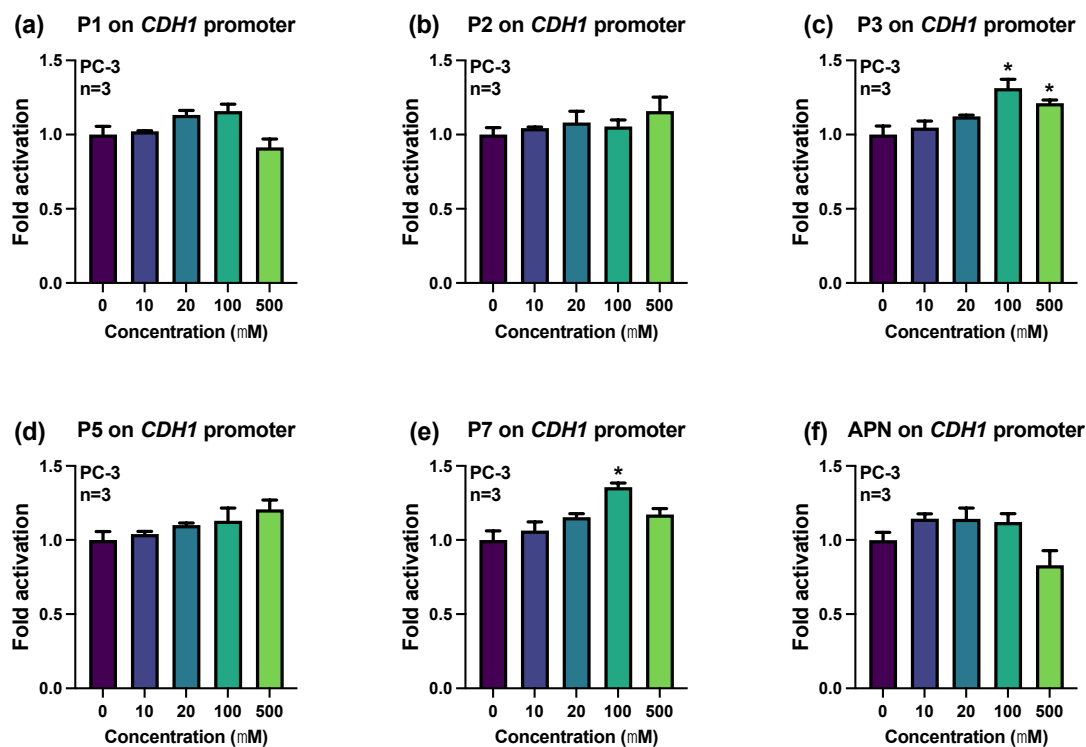


Figure 5. Effects of the indicated molecules on the activation of the *CDH1* promoter. PC-3 prostate cancer cells were transfected with a luciferase plasmid reporter harboring the human -670 to $+92$ bp *CDH1* promoter upstream of the gene encoding *Firefly* luciferase. Cells were treated with increasing concentrations of the indicated molecules for 6 h. Results for the activation of the *CDH1* promoter following treatments of PC-3 cells with P1 (a), P2 (b), P3 (c), P5 (d), P7 (e), and APN (f) are presented. Results are presented as fold activation over the control (DMSO only) (\pm SEM). A one-way ANOVA was used to analyze data according to the concentrations of indicated molecules, followed by Dunnett's multiple comparison test for significant differences compared to the control ($* p < 0.05$).

2.3. Physicochemical Properties and Drug-likeness Prediction

As shown in Table 1, the ADME (adsorption, distribution, metabolism, and excretion) properties of APN and the investigated analogs (P1–P7) were predicted using SwissADME [28]. APN, analog P1, and analogs P3–P6 are all in agreement with Lipinski's Rule of five [29]. All analogs will have high bioavailability since they have a predicted topological surface area (TSA) below 140 (Table 1). Analog P1, P6, and P7 and APN will have high gastrointestinal absorption (GIA) and no ability to cross the blood–brain barrier except for molecule P7 (Table 1). Analog P2 is the only one to violate Lipinski's Rule of five [29] as its number of hydrogen bond acceptors (HBA) is greater than 5 and its TPS is greater than 140 (Table 1).

Table 1. Absorption, distribution, metabolism, and excretion (ADME) profile of the molecules of interest.

Rule	Physicochemical Properties				Lipophilicity		Pharmacokinetics	
	MW (g/mol)	ROTB (n)	HBA (n)	HBD (n)	TPSA (Å)	CLogP _{o/w}	GIA	BBBP
Rule	<500	≤10	<10	<5	≤140	<5	-	-
P1	290.70	1	4	3	73.83	0.26	High	No
P2	452.84	4	9	6	152.98	−1.23	Low	No
P3	436.84	4	8	5	132.75	−1.16	Low	No
P5	436.84	4	8	5	132.75	−0.84	Low	No
P6	450.87	5	8	4	121.75	−0.42	High	No
P7	274.70	1	3	2	53.60	0.91	High	Yes
APN	290.70	1	4	3	73.83	0.23	High	No

Abbreviations: BBBP, blood–brain barrier permeation; CLog Po/w, logarithm of compound partition coefficient between n-octanol and water; GIA, gastrointestinal absorption; HBA, hydrogen bond acceptors; HBD, hydrogen bond donors; MW, molecular weight; n, number; ROTB, rotatable bonds; TPSA, topological polar surface area.

3. Discussion

Regarding the viability of PC-3 prostate cancer cells in response to treatments with the synthesized pigments, the P1 molecule, bearing a hydroxyl at position 3', appears to be the most promising with reduced viability at concentrations of 100 to 500 μM. However, P1 only increases the activity of the NFκB transcription factor while having no effect on *CDH1* promoter activity. Among the synthesized pigments activating the transcription factors NFκB, CREB, and SOX in PC-3 cells, P7 and its glycosylated analog P3 are promising as these molecules also increase *CDH1* promoter activity. Increased *CDH1* expression in cancer cells reduces their ability to undergo epithelial–mesenchymal transition [30] and consequently, their metastatic potential. Interestingly, the expression of *CDH1* may be activated by SOX17, as suggested in esophageal cancer cells [31]. In addition, SOX17 is also highly expressed in prostate cancer [32].

The constitutive activation of NFκB transcription factors is commonly observed in different types of cancer. During prostate cancer progression, NFκB activation promotes cell survival, tumor invasion, metastatic activity, and chemoresistance [33]. Moreover, constitutive NFκB activation is associated with loss of androgen receptor expression and with an androgen-resistant phenotype of prostate cancer [34]. Thus, the inhibition of NFκB activity by APN could promote the treatment of highly aggressive, chemotherapy-resistant prostate cancers.

Interestingly, APN also decreases the activity of SOX transcription factors in PC-3 prostate cancer cells. However, the inhibitory effects of APN on the activities of NFκB and SOX factors do not translate into a modulation of *CDH1* promoter activity. This suggests that APN may inhibit prostate cancer development by influencing the activity of signaling pathways or transcript factors involved in the tumorigenesis, proliferation, invasion, and/or metastatic activity of cancer cells. Interestingly, APN reduced the viability of HL-60 and HepG2 human cancer cells by more than 40% following treatments of 48 h with concentrations from 100 to 200 μM [35]. In addition, extracts containing APN from *Sorghum bicolor* decreased the viability of different cancer cells, including DU145 and LNCap prostate cancer cells [36]. Furthermore, one extract induced apoptosis of A549 lung cancer cells by decreasing the phosphorylation of the signal transducer and activator of transcription 3 (STAT3) transcription factor and the activation of caspase 3 [36]. However, STAT3 is not expressed in PC-3 cells (*our personal observations*). Thus, further investigation is needed to elucidate the mechanism of action responsible for APN cytotoxicity in prostate cancer cells.

The regulation of *CDH1* expression by the transcription factors SOX, CREB, and NFκB is supported by the presence of DNA regulatory elements enabling their recruitment to the −670 to +92 bp *CDH1* promoter region. Indeed, the *CDH1* promoter contains two SOX DNA regulatory elements at −307 and −177 bp and two NFκB DNA regulatory elements

4.2. Reagents

All starting materials were obtained from commercial suppliers. 4'-hydroxyacetophenone, 4'-methoxyacetophenone, 2, 4-dihydroxybenzaldehyde, 2-hydroxy-4-methoxybenzaldehyde, and chlorotrimethylsilane were purchased from Aldrich-Sigma (Saint-Quentin-Fallavier, France). 2, 4, 6-Trihydroxybenzaldehyde was purchased from Extrasynthese (Rhône, France). 3',4'-Dihydroxyacetophenone and 4-(2',3',4',6'-tetra-O-acetyl- β -D-glucopyranosyloxy)-2-hydroxybenzaldehyde (1) were prepared as reported previously [14].

TLC analyses were performed as described previously [13]. Purifications of intermediates were performed using column chromatography with silica gel 60 (40–63 mm, from Merck (Rahway, NJ, USA)). Pigments were purified from elution on C18 silica gel cartridges (bond elut from Varian (Palo Alto, CA, USA)).

^1H and ^{13}C NMR spectra were recorded on an AscendTM 400 Bruker apparatus at 400.18 MHz (^1H) or 100.62 MHz (^{13}C). Chemical shifts (δ) are in ppm relative to tetramethylsilane using the deuterium signal of the solvent (CDCl_3 , CD_3OD) for calibration. ^1H - ^1H coupling constants (J) are in Hz. The ^1H and ^{13}C NMR spectra were published previously [13].

UPLC-MS analyses were completed using the parameters established previously [13]. $\text{H}_2\text{O}/\text{HCO}_2\text{H}$ (99:1, v/v) (eluent A) and $\text{MeCN}/\text{H}_2\text{O}$ (60:40) + 1% HCO_2H (eluent B) at a flow rate of 0.5 mL min^{-1} were used as the mobile phase. The elution program was as follows: 5–20% B (0–5 min), 20–100% B (5–10 min), 5–100% B (10–11 min), and 5% B (11–14 min). UV-vis absorption spectra were recorded on an Agilent 8453 diode array spectrometer equipped with a magnetically stirred quartz cell (optical path length—1 cm). The temperature in the cell was controlled by means of a water-thermostated bath at 25°C .

HRMS analysis was carried out on a Qstar Elite mass spectrometer (Applied Biosystems SCIEX, Foster City, CA, USA). Mass detection was performed in the positive ESI mode.

UV-vis absorption spectra were recorded on an Agilent 8453 diode array spectrometer equipped with a magnetically stirred quartz cell (optical path length—1 cm). The temperature in the cell was controlled by means of a water-thermostated bath at 25°C .

4.3. Cell Culture

The PC-3 (CRL-1435TM) prostate cancer cell line was obtained from the American Type Culture Collection (Manassas, VA, USA) and cultured in F12K cell culture medium supplemented with 10% fetal bovine serum (Wisent Inc., St-Bruno, QC, Canada) and penicillin/streptomycin sulfate (50 mg/L). Cells were incubated at 37°C and 5% CO_2 .

4.4. Cell Viability Assay

Following treatments of PC-3 cells with increasing concentrations of the indicated molecules for 24 h, the cells were incubated with 0.2 mg/mL resazurin for 4 h at 37°C . Then, cell viability was determined by measuring fluorescence ($\text{Ex} = 550 \text{ nm}$, $\text{Em} = 605$, bandwidth = 10 nm).

4.5. Plasmids and Transfection

The pNF κ B-luc (LR-2001), pCREB-luc (LR-2008), and pSOX5-luc (LR-2090) reporter plasmid constructs harboring six consensus regulatory elements for NF κ B (5'-GGGAATTTCC-3'), three consensus regulatory elements for CREB (5'-TGACGTCA-3'), or four consensus regulatory elements for SOX (5'-TCAACAATCC-3'), respectively, were purchased from Signosis Inc. (Santa Clara, CA, USA). The SOX5 DNA regulatory elements of the pSOX5-luc plasmid can also be recognized by other members of the SOX family. Hence, this plasmid is referred to as pSOX-luc in the remainder of this manuscript. For the pNF κ B-luc plasmid, the inserted sequence can be recognized by RELA, NF κ B1, or NF κ B2 according to the JASPAR database [41]. The human -670 to $+92$ bp *CDH1* promoter/luciferase reporter construct (#42083) was purchased from Addgene (Watertown, MA, USA). For transfections, PC-3 cells were plated in 96-well plates, incubated for 24 h, and transfected using polyethylenimine according to the method described previously [42]. After an incubation of 48 h, cells were

treated with increasing concentrations of the indicated molecules for 6 h, followed by cell lysis and measurement of luciferase activity using a Varioskan luminometer (Thermo Scientific, Waltham, MA, USA).

4.6. In Silico Physicochemical Properties and Drug-likeness Evaluation

The SwissADME web tool [28] was used to assess the physicochemical properties of the synthesized compounds 16a-c and 17a, along with CDC (4) and CAPE (2) as references. Subsequently, the results were filtered based on the Lipinski rule of five, to estimate the potential bioavailability and drug-likeness [29].

4.7. Statistics

Experiments were repeated three or four times, and the data were presented as means \pm S.E.M. Statistical analysis of the data was performed using one-way ANOVA followed by a Dunnett or Holm–Sidak multiple comparisons test using GraphPad Prism version 10.1.0 (GraphPad Software Inc., San Diego, CA, USA). $p < 0.05$ was considered significant.

5. Conclusions

Overall, among the molecules investigated in this study, the synthesized pigment P7 and its glycosylated analog P3 increase the activities of NFkB, CREB, and SOX transcription factors, leading to the upregulation of *CDH1* promoter activity in PC-3 prostate cancer cells. These changes in gene regulation may contribute to the inhibition of the epithelial-to-mesenchymal transition in cancer cells. Also, the natural pigment APN may reduce the viability of PC-3 prostate cancer cells by decreasing the activities of NFkB and SOX transcription factors.

Author Contributions: Conceptualization, N.M., M.T. and L.J.M.; methodology, N.M., M.T. and L.J.M.; validation, N.M., M.T. and L.J.M.; formal analysis, N.M., M.T. and L.J.M.; investigation, N.M., M.R., M.T. and L.J.M.; resources, N.M., M.T. and L.J.M.; writing—original draft preparation, N.M., M.T. and L.J.M.; writing—review and editing, N.M., M.T. and L.J.M.; visualization, M.T. and L.J.M.; supervision, N.M.; funding acquisition, M.T. and L.J.M. All authors have read and agreed to the published version of the manuscript.

Funding: This research was funded by the New Brunswick Health Research Foundation, grant number 2021-BRIDGE-2066 to M.T. and L.J.M.

Institutional Review Board Statement: Not applicable.

Informed Consent Statement: Not applicable.

Data Availability Statement: The original contributions presented in this study are included in this article. Further inquiries can be directed to the corresponding author.

Conflicts of Interest: The authors declare no conflicts of interest. The funders had no role in the design of this study; in the collection, analyses, or interpretation of data; in the writing of this manuscript; or in the decision to publish the results.

References

1. Yoshida, K.; Mori, M.; Kondo, T. Blue Flower Color Development by Anthocyanins: From Chemical Structure to Cell Physiology. *Nat. Prod. Rep.* **2009**, *26*, 884–915. [[CrossRef](#)] [[PubMed](#)]
2. Galland, S.; Mora, N.; Abert-Vian, M.; Rakotomanomana, N.; Dangles, O. Chemical Synthesis of Hydroxycinnamic Acid Glucosides and Evaluation of Their Ability to Stabilize Natural Colors via Anthocyanin Copigmentation. *J. Agric. Food Chem.* **2007**, *55*, 7573–7579. [[CrossRef](#)] [[PubMed](#)]
3. Willstätter, R.; Everest, A.E. Untersuchungen Über Die Anthocyane. I. Über Den Farbstoff Der Kornblume. *Justus Liebigs Ann. Chem.* **1913**, *401*, 189–232. [[CrossRef](#)]
4. Asen, S.; Stewart, R.N.; Norris, K.H. Anthocyanin, Flavonol Copigments, and pH Responsible for Larkspur Flower Color. *Phytochemistry* **1975**, *14*, 2677–2682. [[CrossRef](#)]
5. Tsuda, T. Dietary Anthocyanin-Rich Plants: Biochemical Basis and Recent Progress in Health Benefits Studies. *Mol. Nutr. Food Res.* **2012**, *56*, 159–170. [[CrossRef](#)]

6. Awika, J.M.; Rooney, L.W.; Waniska, R.D. Anthocyanins from Black Sorghum and Their Antioxidant Properties. *Food Chem.* **2005**, *90*, 293–301. [[CrossRef](#)]
7. Mazza, G.; Brouillard, R. Color Stability and Structural Transformations of Cyanidin 3,5-Diglucoside and Four 3-Deoxyanthocyanins in Aqueous Solutions. *J. Agric. Food Chem.* **1987**, *35*, 422–426. [[CrossRef](#)]
8. Pina, F.; Melo, M.J.; Laia, C.A.; Parola, A.J.; Lima, J.C. Chemistry and Applications of Flavylium Compounds: A Handful of Colours. *Chem. Soc. Rev.* **2012**, *41*, 869–908. [[CrossRef](#)]
9. Yang, L.; Dykes, L.; Awika, J.M. Thermal Stability of 3-Deoxyanthocyanidin Pigments. *Food Chem.* **2014**, *160*, 246–254. [[CrossRef](#)]
10. Awika, J.M.; Rooney, L.W. Sorghum Phytochemicals and Their Potential Impact on Human Health. *Phytochemistry* **2004**, *65*, 1199–1221. [[CrossRef](#)]
11. Carbonneau, M.-A.; Cisse, M.; Mora-Soumille, N.; Dairi, S.; Rosa, M.; Michel, F.; Lauret, C.; Cristol, J.-P.; Dangles, O. Antioxidant Properties of 3-Deoxyanthocyanidins and Polyphenolic Extracts from Côte d’Ivoire’s Red and White Sorghums Assessed by ORAC and in Vitro LDL Oxidisability Tests. *Food Chem.* **2014**, *145*, 701–709. [[CrossRef](#)] [[PubMed](#)]
12. Taylor, J.R.; Belton, P.S.; Beta, T.; Duodu, K.G. Increasing the Utilisation of Sorghum, Millets and Pseudocereals: Developments in the Science of Their Phenolic Phytochemicals, Biofortification and Protein Functionality. *J. Cereal Sci.* **2014**, *59*, 257–275. [[CrossRef](#)]
13. Al Bittar, S.; Mora, N.; Loonis, M.; Dangles, O. A Simple Synthesis of 3-Deoxyanthocyanidins and Their O-Glucosides. *Tetrahedron* **2016**, *72*, 4294–4302. [[CrossRef](#)]
14. Mora-Soumille, N.; Al Bittar, S.; Rosa, M.; Dangles, O. Analogs of Anthocyanins with a 3', 4'-Dihydroxy Substitution: Synthesis and Investigation of Their Acid-Base, Hydration, Metal Binding and Hydrogen-Donating Properties in Aqueous Solution. *Dye. Pigment.* **2013**, *96*, 7–15. [[CrossRef](#)]
15. Bushweller, J.H. Targeting Transcription Factors in Cancer—From Undruggable to Reality. *Nat. Rev. Cancer* **2019**, *19*, 611–624. [[CrossRef](#)]
16. Lasko, L.M.; Jakob, C.G.; Edalji, R.P.; Qiu, W.; Montgomery, D.; Digiammarino, E.L.; Hansen, T.M.; Risi, R.M.; Frey, R.; Manaves, V.; et al. Discovery of a Selective Catalytic P300/CBP Inhibitor That Targets Lineage-Specific Tumours. *Nature* **2017**, *550*, 128–132. [[CrossRef](#)]
17. Grimm, D.; Bauer, J.; Wise, P.; Krüger, M.; Simonsen, U.; Wehland, M.; Infanger, M.; Corydon, T.J. The Role of SOX Family Members in Solid Tumours and Metastasis. *Semin. Cancer Biol.* **2020**, *67*, 122–153. [[CrossRef](#)]
18. Thomas-Jardin, S.E.; Dahl, H.; Nawas, A.F.; Bautista, M.; Delk, N.A. NF- κ B Signaling Promotes Castration-Resistant Prostate Cancer Initiation and Progression. *Pharmacol. Ther.* **2020**, *211*, 107538. [[CrossRef](#)]
19. Yagi, T.; Takeichi, M. Cadherin Superfamily Genes: Functions, Genomic Organization, and Neurologic Diversity. *Genes. Dev.* **2000**, *14*, 1169–1180. [[CrossRef](#)]
20. Tran, N.L.; Nagle, R.B.; Cress, A.E.; Heimark, R.L. N-Cadherin Expression in Human Prostate Carcinoma Cell Lines. An Epithelial-Mesenchymal Transformation Mediating Adhesion with Stromal Cells. *Am. J. Pathol.* **1999**, *155*, 787–798. [[CrossRef](#)]
21. Birchmeier, W.; Behrens, J. Cadherin Expression in Carcinomas: Role in the Formation of Cell Junctions and the Prevention of Invasiveness. *Biochim. Biophys. Acta* **1994**, *1198*, 11–26. [[CrossRef](#)]
22. Luo, J.; Lubaroff, D.M.; Hendrix, M.J. Suppression of Prostate Cancer Invasive Potential and Matrix Metalloproteinase Activity by E-Cadherin Transfection. *Cancer Res.* **1999**, *59*, 3552–3556. [[PubMed](#)]
23. Pattabiraman, D.R.; Bierie, B.; Kober, K.I.; Thiru, P.; Krall, J.A.; Zill, C.; Reinhardt, F.; Tam, W.L.; Weinberg, R.A. Activation of PKA Leads to Mesenchymal-to-Epithelial Transition and Loss of Tumor-Initiating Ability. *Science* **2016**, *351*, aad3680. [[CrossRef](#)] [[PubMed](#)]
24. Min, C.; Eddy, S.F.; Sherr, D.H.; Sonenshein, G.E. NF- κ B and Epithelial to Mesenchymal Transition of Cancer. *J. Cell Biochem.* **2008**, *104*, 733–744. [[CrossRef](#)]
25. Wegner, M. All Purpose Sox: The Many Roles of Sox Proteins in Gene Expression. *Int. J. Biochem. Cell Biol.* **2010**, *42*, 381–390. [[CrossRef](#)]
26. Moreno, P.; Fexova, S.; George, N.; Manning, J.R.; Miao, Z.; Mohammed, S.; Muñoz-Pomer, A.; Fullgrabe, A.; Bi, Y.; Bush, N.; et al. Expression Atlas Update: Gene and Protein Expression in Multiple Species. *Nucleic Acids Res.* **2022**, *50*, D129–D140. [[CrossRef](#)] [[PubMed](#)]
27. Chuang, K.-T.; Chiou, S.-S.; Hsu, S.-H. Recent Advances in Transcription Factors Biomarkers and Targeted Therapies Focusing on Epithelial-Mesenchymal Transition. *Cancers* **2023**, *15*, 3338. [[CrossRef](#)]
28. Daina, A.; Michielin, O.; Zoete, V. SwissADME: A Free Web Tool to Evaluate Pharmacokinetics, Drug-Likeness and Medicinal Chemistry Friendliness of Small Molecules. *Sci. Rep.* **2017**, *7*, 42717. [[CrossRef](#)] [[PubMed](#)]
29. Lipinski, C.A.; Lombardo, F.; Dominy, B.W.; Feeney, P.J. Experimental and Computational Approaches to Estimate Solubility and Permeability in Drug Discovery and Development Settings. *Adv. Drug Deliv. Rev.* **2001**, *46*, 3–26. [[CrossRef](#)]
30. Montanari, M.; Rossetti, S.; Cavaliere, C.; D’Aniello, C.; Malzone, M.G.; Vanacore, D.; Di Franco, R.; La Mantia, E.; Iovane, G.; Piscitelli, R.; et al. Epithelial-Mesenchymal Transition in Prostate Cancer: An Overview. *Oncotarget* **2017**, *8*, 35376–35389. [[CrossRef](#)]
31. Li, W.; Wu, D.; Niu, Z.; Jiang, D.; Ma, H.; He, H.; Zuo, X.; Xie, X.; He, Y. 5-Azacytidine Suppresses EC9706 Cell Proliferation and Metastasis by Upregulating the Expression of SOX17 and CDH1. *Int. J. Mol. Med.* **2016**, *38*, 1047–1054. [[CrossRef](#)]

32. Du, Z.; Li, L.; Sun, W.; Zhu, P.; Cheng, S.; Yang, X.; Luo, C.; Yu, X.; Wu, X. Systematic Evaluation for the Influences of the SOX17/Notch Receptor Family Members on Reversing Enzalutamide Resistance in Castration-Resistant Prostate Cancer Cells. *Front. Oncol.* **2021**, *11*, 607291. [[CrossRef](#)]
33. Staal, J.; Beyaert, R. Inflammation and NF- κ B Signaling in Prostate Cancer: Mechanisms and Clinical Implications. *Cells* **2018**, *7*, 122. [[CrossRef](#)]
34. Bishop, J.L.; Davies, A.; Ketola, K.; Zoubeidi, A. Regulation of Tumor Cell Plasticity by the Androgen Receptor in Prostate Cancer. *Endocr. Relat. Cancer* **2015**, *22*, R165–R182. [[CrossRef](#)]
35. Shih, C.-H.; Siu, S.-O.; Ng, R.; Wong, E.; Chiu, L.C.M.; Chu, I.K.; Lo, C. Quantitative Analysis of Anticancer 3-Deoxyanthocyanidins in Infected Sorghum Seedlings. *J. Agric. Food Chem.* **2007**, *55*, 254–259. [[CrossRef](#)]
36. Owumi, S.E.; Kazeem, A.I.; Wu, B.; Ishokare, L.O.; Arunsi, U.O.; Oyelere, A.K. Apigeninidin-Rich Sorghum Bicolor (L. Moench) Extracts Suppress A549 Cells Proliferation and Ameliorate Toxicity of Aflatoxin B1-Mediated Liver and Kidney Derangement in Rats. *Sci. Rep.* **2022**, *12*, 7438. [[CrossRef](#)]
37. Watson, M.J.; Berger, P.L.; Banerjee, K.; Frank, S.B.; Tang, L.; Ganguly, S.S.; Hostetter, G.; Winn, M.; Miranti, C.K. Aberrant CREB1 Activation in Prostate Cancer Disrupts Normal Prostate Luminal Cell Differentiation. *Oncogene* **2021**, *40*, 3260–3272. [[CrossRef](#)]
38. Lin, Y.-W.; Tsao, C.-M.; Yu, P.-N.; Shih, Y.-L.; Lin, C.-H.; Yan, M.-D. SOX1 Suppresses Cell Growth and Invasion in Cervical Cancer. *Gynecol. Oncol.* **2013**, *131*, 174–181. [[CrossRef](#)]
39. Wong, S.H.M.; Fang, C.M.; Chuah, L.-H.; Leong, C.O.; Ngai, S.C. E-Cadherin: Its Dysregulation in Carcinogenesis and Clinical Implications. *Crit. Rev. Oncol. Hematol.* **2018**, *121*, 11–22. [[CrossRef](#)]
40. Canel, M.; Serrels, A.; Frame, M.C.; Brunton, V.G. E-Cadherin-Integrin Crosstalk in Cancer Invasion and Metastasis. *J. Cell Sci.* **2013**, *126*, 393–401. [[CrossRef](#)]
41. Rauluseviciute, I.; Riudavets-Puig, R.; Blanc-Mathieu, R.; Castro-Mondragon, J.A.; Ferenc, K.; Kumar, V.; Lemma, R.B.; Lucas, J.; Chèneby, J.; Baranasic, D.; et al. JASPAR 2024: 20th Anniversary of the Open-Access Database of Transcription Factor Binding Profiles. *Nucleic Acids Res.* **2024**, *52*, D174–D182. [[CrossRef](#)]
42. Ghouili, F.; Martin, L.J. Cooperative Regulation of Gja1 Expression by Members of the AP-1 Family cJun and cFos in TM3 Leydig and TM4 Sertoli Cells. *Gene* **2017**, *635*, 24–32. [[CrossRef](#)]

Disclaimer/Publisher’s Note: The statements, opinions and data contained in all publications are solely those of the individual author(s) and contributor(s) and not of MDPI and/or the editor(s). MDPI and/or the editor(s) disclaim responsibility for any injury to people or property resulting from any ideas, methods, instructions or products referred to in the content.